REPORT NUMBER
LAPS 45
SAI-78-857-LJ
SEPTEMBER 1978

UC-20

MASTER

LABORATORY FOR APPLIED PLASMA STUDIES

DRIFT WAVE STABILITY AND TRANSPORT THEORY

by

N. A. Krall, S. Hamasaki, J. B. McBride, R. E. Aamodt, et al.

SCIENCE
APPLICATIONS
INCORPORATED

REPORT NUMBER
LAPS 45
SAI-78-857-LJ
SEPTEMBER 1978

UC-20

DRIFT WAVE STABILITY AND TRANSPORT THEORY

by

N. A. Krall, S. Hamasaki, J. B. McBride, R. E. Aamodt, et al.

DRIFT WAVE STABILITY AND TRANSPORT THEORY

N. A. Krall, S. Hamasaki, J. B. McBride
Science Applications, Inc., La Jolla, California 92037

N. T. Gladd, P. H. Ng, and H. H. Chen
University of Maryland, College Park, Maryland 20742

J. D. Huba
Naval Research Laboratory, Washington, DC 20375

R. C. Davidson
Office of Fusion Energy, Department of Energy
Washington, DC 20545

R. E. Aamodt, Y. C. Lee, C. S. Liu, D. R. Nicholson,
M. N. Rosenbluth
Science Applications, Inc., Boulder, Colorado 80302

D. Chernin
Institute for Advanced Study, Princeton, New Jersey 08540

ABSTRACT

The linear properties of lower hybrid, drift cyclotron, and drift cyclotron loss cone instabilities are calculated including shear, beta, and distribution function effects. Transport runs including these effects are carried out for experiment-sized and reactor-sized devices. Nonlinear effects on the DC mode due to frequency and wavenumber shifts are calculated.

1. INTRODUCTION

It is generally accepted[1] that microinstabilities affect both the heating and loss (of particles and heat) in many plasma containment devices. The modeling and prediction of the behavior of linear theta pinch, reversed field pinch (RFP), imploding liner, and magnetic mirror machines all require knowledge of the linear and nonlinear behavior of the lower hybrid (LH), ion cyclotron drift (DC), and drift cyclotron loss cone modes (DCLC), including such realistic features as finite beta, magnetic shear, and the full set of particle and temperature gradients. In this paper, we give many of these properties (Sec. 2) and show how they affect the time evolution of various experiments (Sec. 3). Further, we formulate and examine the effects of the nonlinear frequency shift on the drift cyclotron mode (Maxwellian) and determine the spatial and temporal evolution of the spectrum of such modes in a flute approximation (Sec. 4). The latter calculation bears on mirror loss cones with a warm plasma stream.

2. LINEAR PROPERTIES OF LH, DC, AND DCLC INSTABILITIES

The linear theory of these three modes have been widely discussed in the low β, no-shear, constant temperature limit.[1] In summary, their properties in this limit are (L_n is the scale size, a_i the ion gyroradius)

$$\mathrm{LH}\left(L_n/a_i \lesssim 1\right) \quad \gamma \sim \omega_o \sim \left(\omega_{ce}\omega_{ci}\right)^{\frac{1}{2}}\left(1+\omega_{ce}{}^2/\omega_{pe}{}^2\right)^{\frac{1}{2}} \equiv \omega_H$$

$$\mathrm{LH}\left[\left(M_i/M_e\right)^{\frac{1}{4}} > L_n/a_i > 1\right] \quad \omega_o \sim \omega_H\left(a_i/L_n\right);\ \gamma \sim \omega_o\left(a_i/L_n\right)$$

$$\mathrm{DC}\left[\left(M_i/M_e\right)^{\frac{1}{2}} > L_n/a_i > \left(M_i/M_e\right)^{\frac{1}{4}}\right] \quad \omega_o \sim \ell\omega_{ci} \sim kV_D;\ \gamma \sim \omega_o\left(M_e/M_i\right)^{\frac{1}{2}} \ .$$

In this section, we extend these conditions to include various magnetic geometries, and distribution function effects, using both analytic and numerical solutions of the dispersion relation, extended for non-local effects to the form[2] $A\varphi'' + Q(\omega, k, r)\varphi = 0$, and for finite β effects to a 2 x 2 dispersion matrix.[2] The details of the analytic and numerical techniques, along with further graphs and results are presented elsewhere.[3-7] This section summarizes the results. The definition of shear and notation are standard.[3,6]

2.1 Lower Hybrid with Shear, Weak Inhomogeneity[3]

In the low β limit, an analytic estimate of shear stabilization can be made. The result is LH is stable if

$$\frac{L_s}{L_n} < \frac{4L_n}{a_i}\left(1+\frac{\omega_{ce}{}^2}{\omega_{pe}{}^2}\right)^{\frac{1}{2}} \quad \text{if} \quad \frac{T_e}{T_i} \ll 1+\omega_{ce}{}^2/\omega_{pe}{}^2 \qquad (1)$$

$$\frac{L_s}{L_n} < \frac{L_n}{a_i} \frac{\left(1 + T_e/T_i\right)^2}{T_e/T_i} \quad \text{if} \quad \frac{T_e}{T_i} >> 1 + \omega_{ce}^2/\omega_{pe}^2 \qquad (2)$$

The last mode to stabilize has wavenumber $K^2 a_e^2 = (T_e/T_i(1 + T_e/T_i + \omega_c^2/\omega_{pe}^2$.

To include finite β and also the effect of strong inhomogeneities $[1 \geq a_i/L_n > (m_e/m_i)^{\frac{1}{2}}]$ requires numerical analysis. We present two examples.

2.2 Lower Hybrid with Shear and Finite $\beta_i (T_e/T_i \to 0)$[6]

The analysis uses a fully electromagnetic, non-local, Weber-like dispersion equation to include finite ion β as well as magnetic shear. The results of numerical integration of this equation are shown in Fig. 1a. Although for shear much too weak to stabilize the LH mode increasing β_i tends to decrease the growth rate, the ultimate effect is that increasing β_i somewhat increases the shear needed to stabilize. The curve below $a_i/L_n = 1$ agrees with the analytic calculation Eq. (1).

2.3 Lower Hybrid with Shear, Strong Inhomogeneity[6]

As shown in Fig. 1b, numerical integration of the $\beta = 0$ dispersion equation shows that increasing T_e/T_i reduces the amount of shear needed to stabilize in the weak gradient limit, in agreenent with Eq. (1) - Eq. (2);

however, increasing T_e/T_i increases the shear for stability in the strong gradient limit.

2.4 Lower Hybrid with Temperature Gradients[4]

The problem of linear stability of the LH mode in low β can be generalized to include temperature gradients. Such a calculation has been carried out and the results are, in summary: the LH mode is unstable only for wavelengths such that ($\eta_{Tj} = d\ell nT_j/d\ell n\, n$)

$$1 > b_e > \frac{T_e}{2T_i} \frac{\eta_{Ti}}{1 - \frac{1}{2}\eta_{Ti}} \left(1 + \frac{\omega_{ce}^2}{\omega_{pe}^2}\right)^{-1} \tag{3}$$

$$b_e^{\frac{1}{2}} > \frac{T_e}{T_i\sqrt{2\pi}} \frac{\left(1 - \frac{1}{2}\eta_{Te}\right)}{\left(1 - \frac{1}{2}\eta_{Ti}\right)\left(1 + T_e/T_i + b_e\omega_{ce}^2/\omega_{pe}^2\right)} > 1 \tag{4}$$

Note that whereas without ion temperature gradients ($\eta_{Ti} \to 0$) all long wavelength modes are unstable, the unstable spectrum is reduced for η_{Ti} positive. Eqs. (3-4) are also necessary for the DC mode, where $\omega = \omega_{ci} = kV_D$ determines the wavenumber.

2.5 DC with Shear[3]

In a calculation similar to that described for the LH mode, we have obtained an analytic solution to the non-local dispersion equation, by

solving the Weber-like equation for the perturbed potential $A\varphi''$ $+ (B-Cx^2)\varphi = 0$, where $B(x_o, \omega, k)$ is the local dispersion relation. In this case, in contrast to LH, shear reduces the growth rate rather than stabilizing the mode. The condition for shear to reduce the growth of all wavelengths of the DC modes is

$$\frac{L_s}{L_n} < \left(1 + \frac{T_e}{T_i}\right)^{\frac{1}{2}} \left(\frac{M_i}{M_e}\right)^{\frac{1}{2}} \left(\frac{a_i}{L_n}\right)^{\frac{1}{2}} \qquad (5)$$

(A somewhat weaker value of shear affects the very short wavelengths, $ka_i >> 1.$) Since the LH mode can be shown to merge with the DC mode for $(L_n/a_i) \cong (m_i/m_e)^{\frac{1}{4}}$, Eq. (5) is clearly the same as the condition for stabilizing LH modes, Eq. (1) at this value of L_n. Note also that the linear stability condition $L_n < a_i(m_i/m_e)^{\frac{1}{2}}$ bounds the righthand side of Eq. (5).

2.6 DC with Finite β

A detailed numerical study of the linear dispersion matrix for DC instabilities, including electromagnetic perturbations, allows study of this mode for finite $\beta = 8\pi n(T_e+T_i)/B^2$, as well as the transition to the LH mode discussed above. The results are shown in Fig. 2a and Fig. 2b. For

$\beta << (m_e/m_i)^{\frac{1}{4}}$ all effects are small. For larger values, β becomes a significant stabilizing effect, due particularly to resonant ∇B orbit modifications from finite β as $\omega/kV_B \to 1$, where $V_B \cong (cT/eBL_n)\beta$. Fig. 2a and Fig. 2b show the reduction of the growth rate for various T_e/T_i and for $T_e = 0$. The double curve is because $\gamma = \gamma_{max}$ for two different values of k_y, when β gets sufficiently large. As usual electromagnetic effects prevent the "self-dug well" of the electrostatic term from stabilizing the mode. Similar though less detailed results have been obtained analytically in an earlier publication. We conclude that although finite β slows the instability, it may still persist until diffusion broadens the profile to the linear stability limit $a_i/L_n \simeq (m_e/m_i)^{\frac{1}{2}}$. In a sufficiently large device, this may be unimportant compared with classical effects. More details are contained elsewhere.[7]

2.7 DCLC with Warm Plasma[5]

Although linear theory predicts that the DCLC mode in a mirror machine will be unstable over a broad band of frequency and wavenumber,[9] experimental observation indicates only narrow bands of instability at the lowest harmonics of the ion cyclotron frequency.[10] A detailed linear analysis is made of the transformation of the DCLC instability into the DC instability as the loss-cone of the ion distribution is filled by a warm

Maxwellian component.[5] In particular the loss cone distribution is modeled by the difference of two Maxwellians with different temperatures $T_H = m_i V_H^2/2$, $T_h = m_i V_h^2/2$ and the warm component by a Maxwellian with temperature $T_w = m_i V_w^2/2$ with Δ the relative fraction of warm component. In general, it is found that the addition of warm plasma ($\Delta \neq 0$) reduces the growth rate of the DCLC and breaks the broad band wavenumber spectrum into a discrete banded structure when $\gamma \lesssim \omega_{ci}$. The detailed features of the spectrum are strongly dependent on the parameters, Δ, T_h/T_H, T_w/T_H characterizing the ion equilibrium. A particularly interesting result is that when the ion velocity distribution is "doubled humped," some parametric combinations (e.g., $a_{iH}/L_N = 0.2$, $\Delta = 0.025$, $T_h/T_H = 0.05$, $T_w/T_H = 0.025$) result in the lowest unstable harmonic having the largest linear growth rate. This result is consistent with experimental observations and agrues that these persistent observations of only the lowest harmonics may possibly be explained, linearly, by means of a partially filled loss cone. Further details, including the effects of temperature gradients and warm plasma component on the instability threshold condition, may be found in Ref. 5.

3. MODELING OF SHEAR- AND BETA-STABILIZED PLASMAS

In order to determine the practical importance of many of the effects discussed above, we have included those results for the LH and

DC instabilities, including finite β and shear effects, in a simulation of this effect on cross field plasma diffusion. We want to determine (a) the necessity of using realistic linear stability estimates and (b) the time evolution of a system in which only part (usually the central part) of the profile is stabilized by these effects. Further, we try to show whether the instabilities will produce the same results in a large, reactor-size device as in a smaller laboratory experiment. Fig. 4a shows a plasma of experimental size which is, at $t = 0$, β-stabilized except near the boundary. By 1 ms the stable region has eroded away and the plasma is nearly lost, showing that finite β stabilization is not very persistent in this configuration. In contrast, a partially shear stabilized case is shown in Fig. 4b of the ZT-1 type configuration, at $t = 0$ and at 1 ms. For contrast $n(t = 1$ ms) is also shown in a calculation neglecting shear stabilization. Note that shear seems a much more persistent stabilizing mechanism than finite β. The other side of the coin is that ZT cannot tolerate too much profile change without losing MHD stability. Finally, Fig. 5a and Fig. 5b show the same calculation as in Fig. 4a and Fig. 4b, but on a reactor-size scale. The finite β system (Fig. 5a) is still eroding, but the rate has been considerably scaled down. The ZT-40 example (Fig. 5b) exhibits little diffusion at all on this time scale. Work in progress will include longer runs and comparison with MHD stability conditions.

4. NONLINEAR THEORY

While drift-unstable ion cyclotron waves (DC) are expected to reduce the containment properties in any magnetic configurations, they are particularly important in mirror devices where the breakdown of adiabaticity can induce rapid particle end losses and where their existence has, in fact, been observed to be correlated with containment degradation.[10,11] As it has been established[12] that particle containment in a mirror trap including DC waves critically depends on the spectrum and amplitude, nonlinear calculations are important to obtain the saturated spectrum characteristics so that a fundamental understanding of mirror machine containment and its extrapolation to larger, hotter devices can be synthesized. In order to model the mirror loss cone plus injected warm plasma stream, we examine the effects of the nonlinear frequency shift on the DC instability (Maxwellian velocity distribution) and determine the spatial and temporal evolution of the spectrum of such modes in a strictly flute approximation.

It has been shown[13-16] that for fixed wavenumber of the ion gyrofrequency is effectively nonlinearly shifted by the ion cyclotron wave which thereby detunes the resonance $\omega \cong \omega_{ci} \cong kV_D$. This stabilizes the DC instability[16] when the nonlinear frequency shift is comparable to the linear growth rate. Since, however, a wavenumber

shift might again allow the proper resonance for instability, we here determine these shifts self-consistently.

Consider the DC instability in an inhomogeneous plasma with a density profile given by $N = N_o(1 + Y/L)$. The electrostatic wave potential is assumed to be of the form $\varphi(x, t) = \Phi(x, t)\exp i(kx-\omega t)$ where Φ is the slowly varying amplitude and x is the direction of the ion diamagnetic drift $\vec{V}_D = (cT_i/eB^2N)\ \vec{B} \times \nabla N$. We examine only the resonant cases of $\omega \approx \omega_{Di} \simeq n\omega_{ci}$. To obtain the effects of the nonlinear frequency and wavenumber shift, we solve the Vlasov equation to the third order in $e\varphi$ and find the resonant ion density fluctuation is

$$n_3 = \frac{\alpha N_o e\varphi}{T_i}\left(\frac{\omega_{xi} - n\omega_{ci}}{\omega - n\omega_{ci}}\right)\Phi^2; \quad \alpha = \frac{8n^2e^2k^2/MT}{\pi^2(\omega-n\omega_{ci})^2(4n^2-1)} \tag{6}$$

The nonresonant terms can be shown to be of order $(ka_i)^{-\frac{1}{2}}$ smaller. The only important electron nonlinearity is the usual quasilinear spatial diffusion effect which can be shown to maintain charge neutrality. The resulting nonlinear wave equation for the slowly varying $\Phi(x, t)$ can then then be obtained as

$$\partial_{tt}\Phi - \partial_{xx}\Phi + \alpha|\Phi|^2\Phi - \gamma^2\Phi = 0 \tag{7}$$

where

$$\gamma = n^2 \omega_{ci} \left(\frac{L}{a_i}\right) \left(\frac{m}{M}\right)^{\frac{1}{2}} \left(1 + \frac{B^2}{4\pi n m c^2}\right)^{\frac{1}{2}}$$

Rescaling $\tau = \gamma t$, $X = \gamma x$ and setting $\Phi = \gamma \alpha^{-\frac{1}{2}} \Phi'$, we normalize Eq. (7) into the standard nonlinear Klein-Gordon equation.[17] For travelling-wave solutions, we may set the dependence of Φ' on τ, X only through $\zeta = X - V\tau$ and then Eq. (7) has standard elliptic function solutions. In the limit of infinite period, there are the solitary-wave solutions, which, however, are either localized but unstable:

$$\Phi = \sqrt{2}\ \mathrm{sech}\left[\zeta / \sqrt{V^2 - 1}\right] (V > 1)$$

or stable but not localized:

$$\tanh\left[\zeta / \sqrt{2(1 - V^2)}\right] \ (|V| < 1).$$

A particular solution of physical interest is the spatially-uniform solution: $\Phi'(X, \tau) = \Phi_0 \exp(-i\omega_0 t)$ with $\omega_0^2 = |\Phi_0|^2 - 1$.

Perturbing this solution with $\delta\Phi \exp[ikX - i(\delta + \omega_0)\tau]$, we find

$$\delta^2 = (\omega_0^2 + \Delta) \pm \sqrt{4\Delta\omega_0^2 + |\Phi_0|^4}$$

where $\Delta = k^2 - 1 + 2|\Phi_0|^2$. As $(\omega_0^2 - \Delta)^2 > |\Phi_0|^4$, this solution is stable to all perturbations. For $\omega_0 = 0$, this is in fact the minimum-

energy state corresponding to being at the bottom of the effective potential well (see below) and we expect that the system would eventually evolve into this state through either radiation or dissipation. This is in fact borne out by the self-similar solution and numerical solution of Eq. (7). With the similarity variable $\xi = \tau^2 - X^2$, Eq. (7) becomes

$$4\xi\left(\xi\Phi_\xi\right)_\xi + \xi\left[|\Phi|^2 - 1\right]\Phi = 0 \tag{8}$$

Setting $\xi = \exp\eta$, Eq. (7) can be cast into the following oscillator equation with nonlinear and "time-varying" spring constant:

$$\frac{d^2\Phi}{d\eta^2} = -\frac{e^\eta}{4}\left[|\Phi|^2 - 1\right]\Phi \tag{9}$$

Eq. (8) is solved numerically and the solution is shown in Fig. 6a. Note that initially the amplitude grows exponentially with the linear growth rate then it saturates and oscillates around $\Phi = 1$ with oscillation frequency $= \sqrt{2}$ in the present dimensionless units. The saturation amplitude for the first harmonic is found to be

$$\frac{e\Phi}{T_i} = \left(\frac{a_i}{L}\right)\left(\frac{m}{M}\right)^{\frac{1}{2}} \tag{10}$$

We have also solved the full space time Eq. (7) numerically, as shown in Fig. 6b. A localized pulse is applied at $x = 0$ at $t = 0$, the pulse propagates outward with dimensionless speed 1.0. At $\tau = 1$,

the response is still growing close to the dimensionless linear growth rate 1.0. However, the curves at $\tau = 4$ and $\tau = 9$ show a nonlinear saturation at the valve 1.0, corresponding to the bottom of the pseudopotential well discussed above. The function $\Phi(X = 0, t)$ as observed in this numerical calculation, not shown, is found to be in precise agreement with the self-similar prediction of Fig. 6a.

Therefore, within the framework of the assumed Maxwellian state, and for the wave numbers in question, we have found very low amplitude saturation of the drift cyclotron waves which is consistent with the experimental observations.[10, 11]

ACKNOWLEDGEMENT

This work was supported by the United States Department of Energy, Contract EY-76-C-03-1018.

REFERENCES

1. Davidson, R. C., Krall, N. A., Nuclear Fusion 17 (1977) 1313.
2. Krall, N. A., "Drift Waves" in Advances in Plasma Physics, Vol. 1 (Wiley, New York 1968).
3. McBride, J. B., Krall, N. A., Nuclear Fusion (1978) in press.
4. McBride, J. B., Hamasaki, S., Phys. Fluids (1978) in press.
5. Ng, P. H., Gladd, N. T., Liu, C. S., University of Maryland Report (to be published) (DCLC finite β), Catto, P., Aamodt, R. Phys. Fluids (in press).
6. Davidson, R. C., Gladd, N. T., Goren, Y., Phys. Fluids 21 (1978) 992.
7. Gladd, N. T., Huba, J. D., Phys. Fluids (submitted) (DC finite β).
8. Krall, N. A., Pearlstein, L. D., Plasma Physics and Controlled Nuclear Fusion Research (IAEA, Vienna 1966) Vol. 1, p. 735.
9. Post, R. F., Rosenbluth, M. N., Phys. Fluids 9 (1966) 730.
10. Turner, W. C., Powers, E. J., Simonen, T. C., Phys. Rev. Lett. 39 (1977) 1087.
11. Coensgen, F. H., Cummins, W. F., Logan, B. G., Molvik, A. W., Nexsen, W. E., Simonen, T. C., Stallard, B. W., Turner, W. C., Phys. Rev. Lett. 35 (1975) 1051; Bagborodov, Y. T., Ioffe, M. S., Kanaev, B. I., Sobolev, R. I., Yushmanov, E. E., in Proceedings

of the Fourth International Conference on Plasma Physics and Controlled Nuclear Fusion Research, Madison, Wisconsin, 1971 (International Atomic Energy Agency, Vienna, Austria, 1972), Vol. 2, p. 641.

12. Aamodt, R. E., Phys. Rev. Lett. 27 (1971) 135; Rosenbluth, M. N., Phys. Rev. Lett. 29 (1972) 408; Timofeev, A. V., Nuclear Fusion 14 (1974) 165; Aamodt, R. E., Byers, J. A., Phys. Rev. Lett. 29 (1972) 1305.

13. Aamodt, R. E., Bodner, S. E., Phys. Fluids 12 (1969) 1471; Aamodt, R. E., Phys. Fluids 17 (1974) 803.

14. Nekrasov, A. K., Nuclear Fusion 14 (1974) 865.

15. Aamodt, R. E., Lee, Y. C., Liu, C. S., Rosenbluth, M. N., Phys. Rev. Lett. 39 (1977) 1660.

16. Zakharov, V., Shabat, A., Zh. Eksp. Teor. Fiz 61 (1972) 118 [Sov. Phys. JETP 34 (1972) 62]; Ablowitz, M., Kaup, D., Newell, A., Segur, H., Stud. Appl. Math. 53 (1974) 249; Makhankov, V. G., Physics Reports 35 (1978) 1.

17. Cohen, B. I., Maron, N., Rognlien, T. D., in the Proceedings of the Annual Controlled Fusion Theory Conference, Gatlinburg, Tenn. (1978) Paper #OA5.

FIGURE CAPTIONS

Figure 1(a) Effect of Magnetic Shear on the LH Drift Instability for Finite β and Cold Electrons.

Figure 1(b) Shear Stabilization of LH for $\beta = 0$ and Various T_e/T_i.

Figure 2(a) Effect of Finite β on the DC Instability for $T_e/T_i = 1$.

Figure 2(b) Effect of Finite β on DC Instability when $T_e = 0$.

Figure 3 Warm Plasma Effects on DCLC Instability for Various Ion Distributions (see text).

Figure 4(a) Time Development of a (partially) β Stabilized Experiment.

Figure 4(b) Time Development of a (partially) Shear Stabilized Experiment.

Figure 5(a) Time Development of a β Stabilized Reactor Prototype.

Figure 5(b) Time Development of a Shear Stabilized Reactor Prototype.

Figure 6(a) Self-Similar Solution of the Nonlinear Klein-Gordon Equation.

Figure 6(b) Space Time Solution of the Nonlinear Partial Differential Equation.

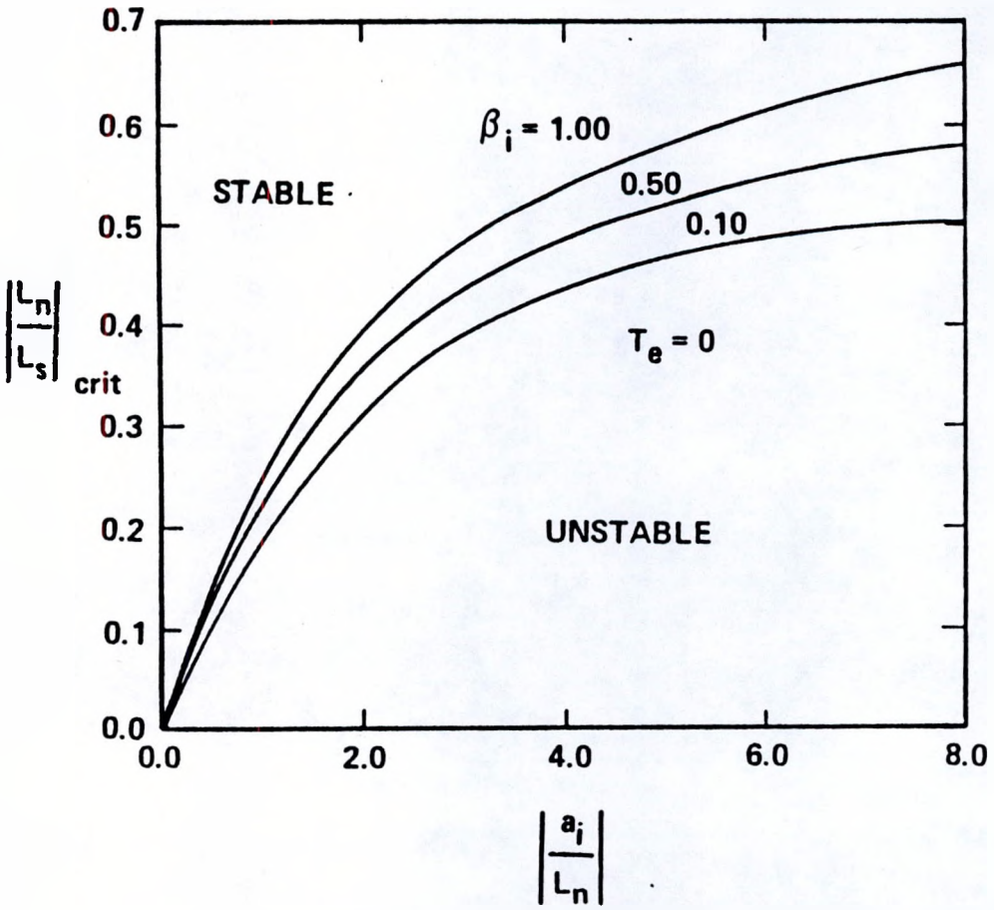

FIGURE 1a

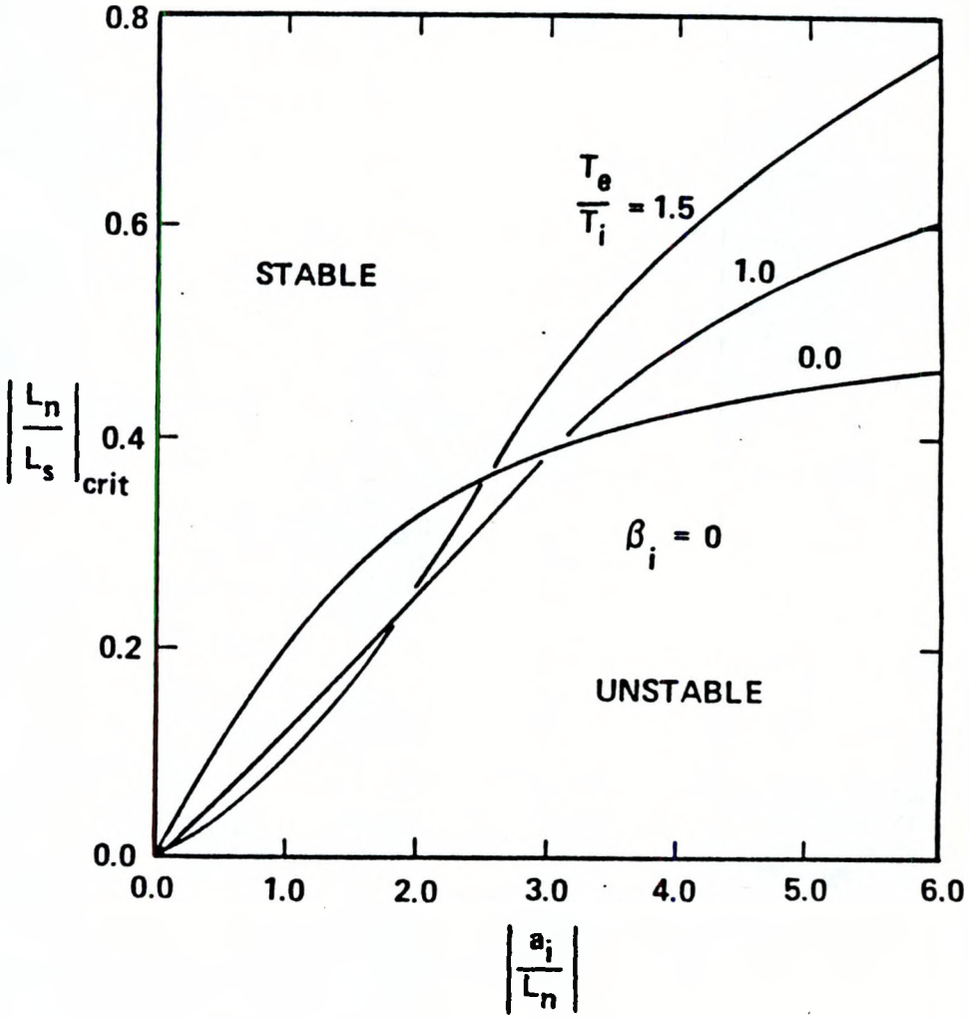

FIGURE 1b

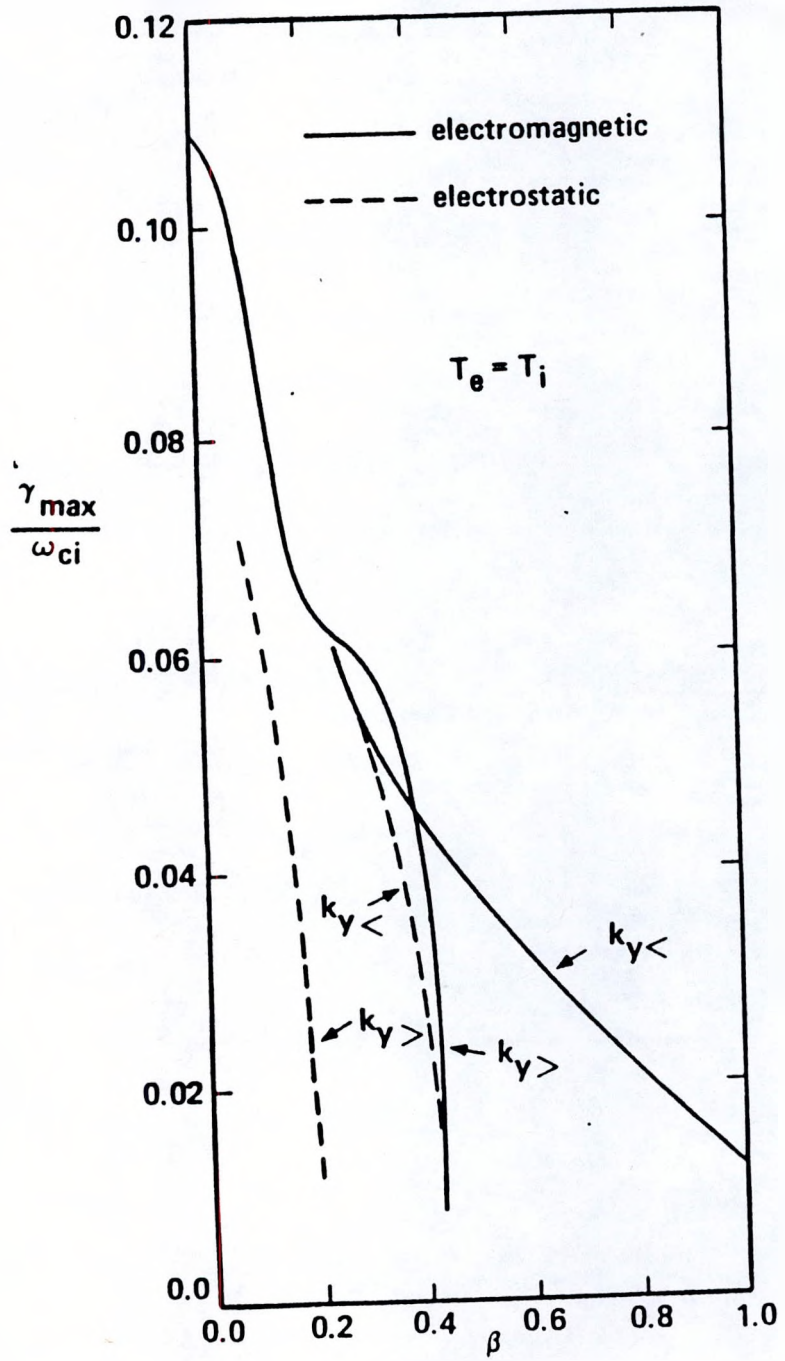

FIGURE 2a

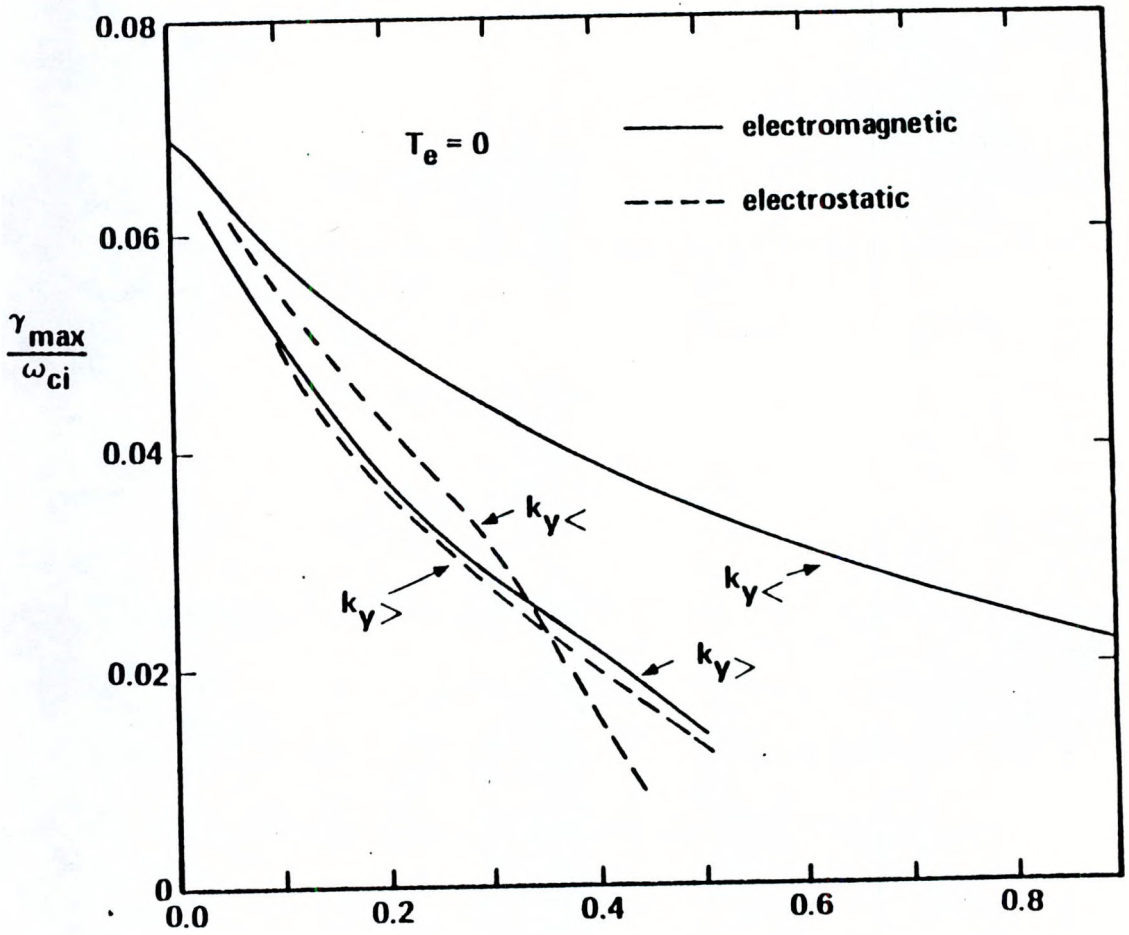

FIGURE 2b

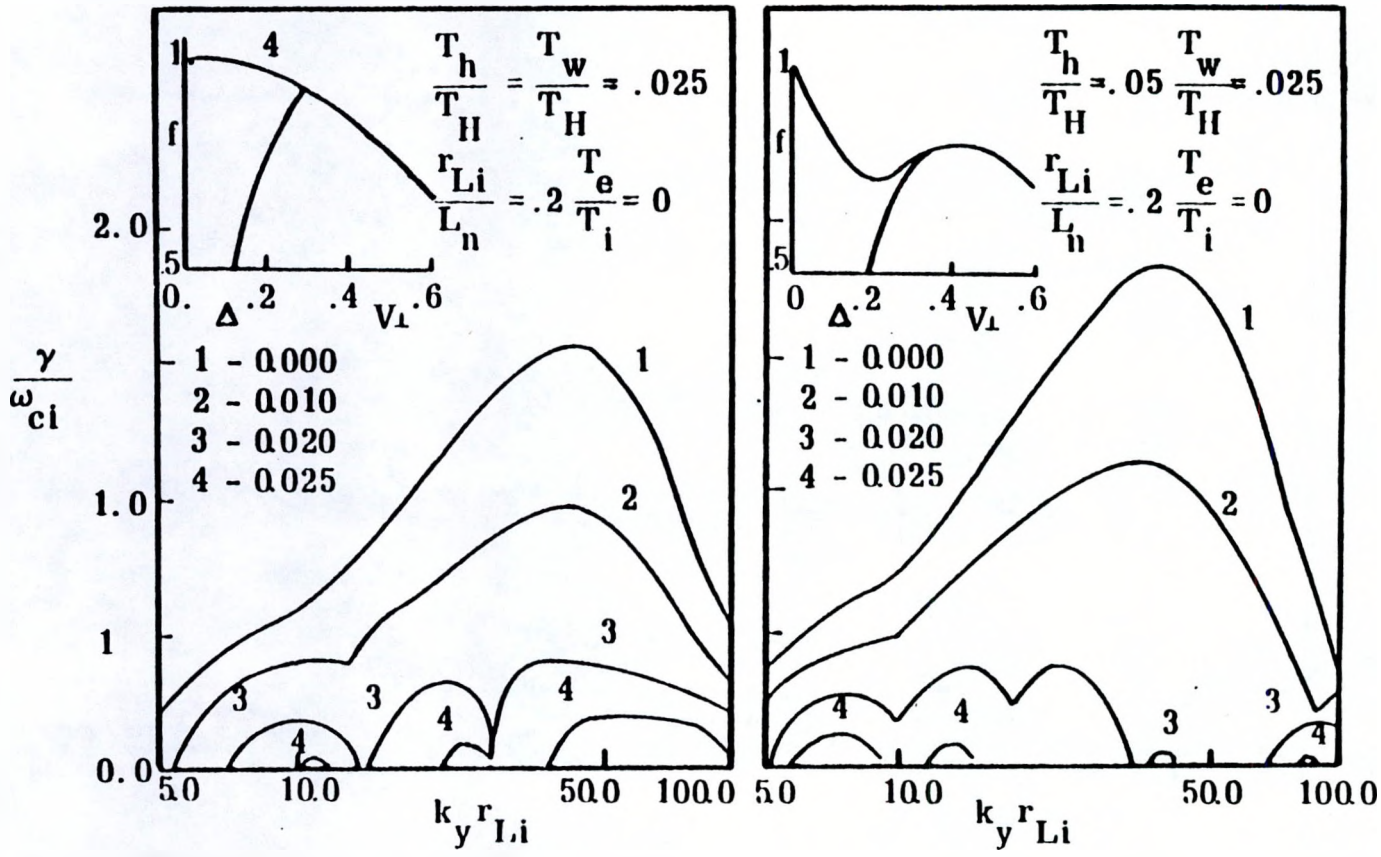

FIGURE 3a

FIGURE 3b

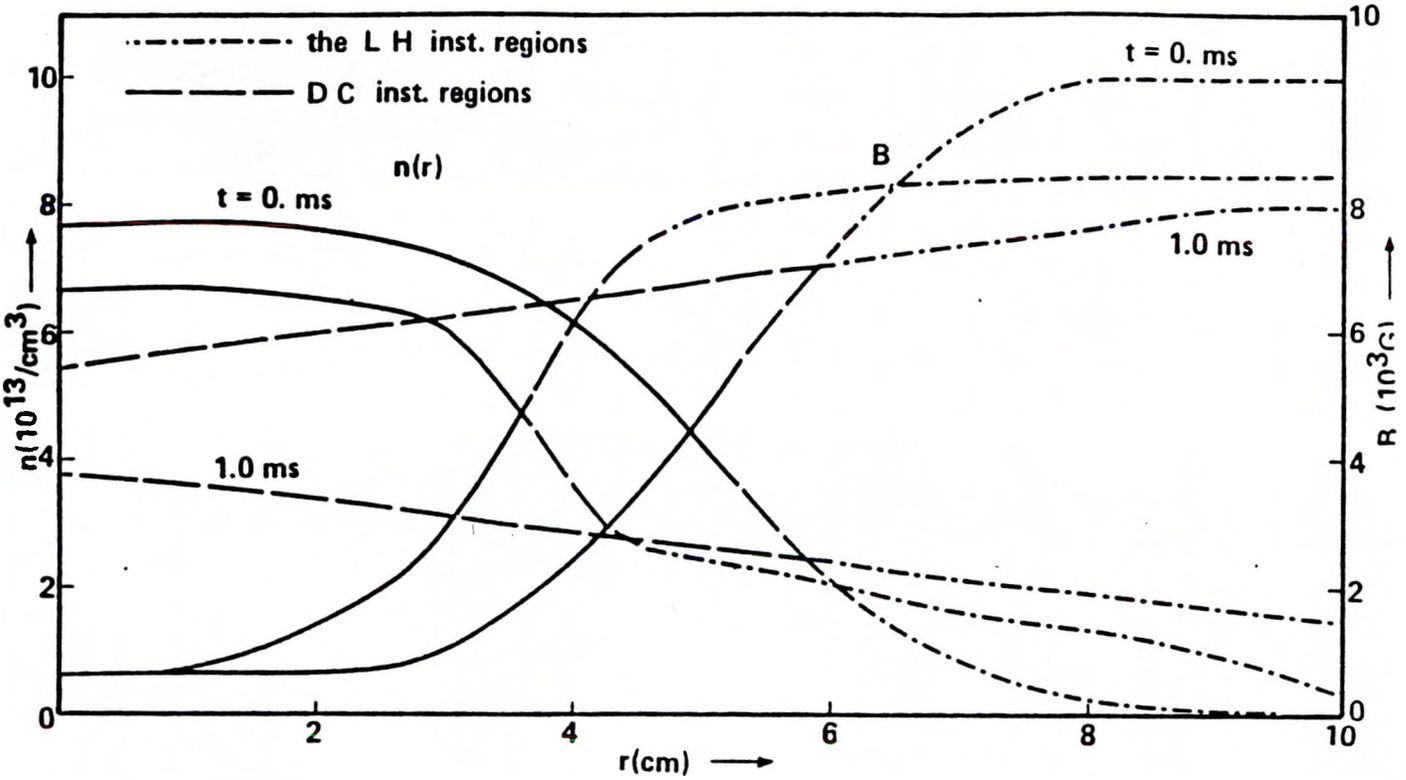

FIGURE 4a

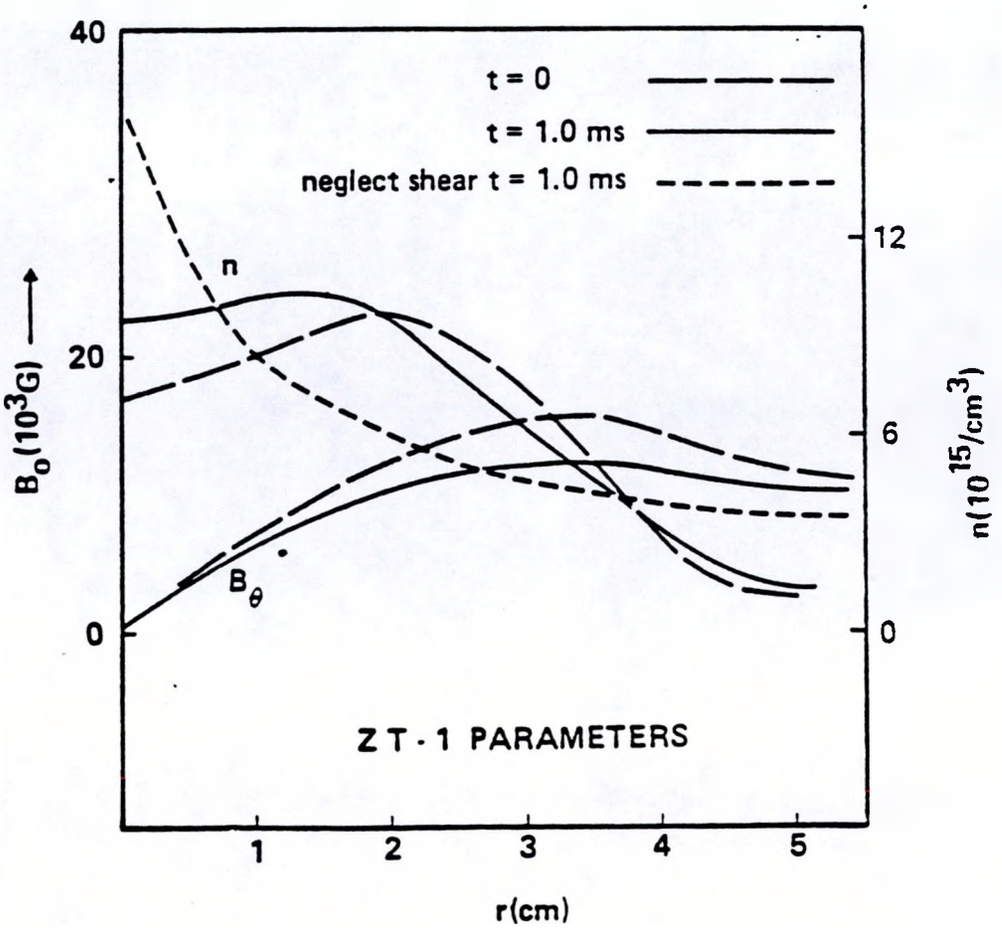

FIGURE 4b

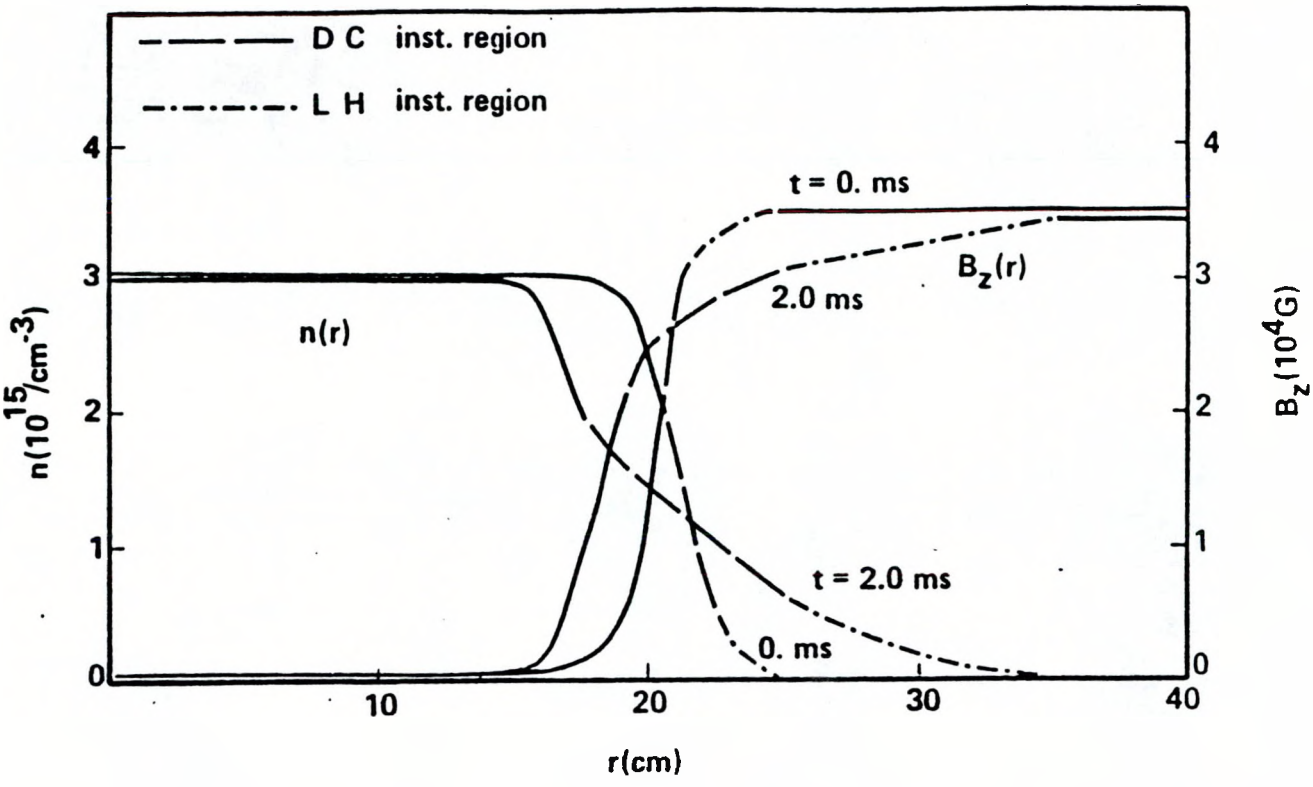

FIGURE 5a

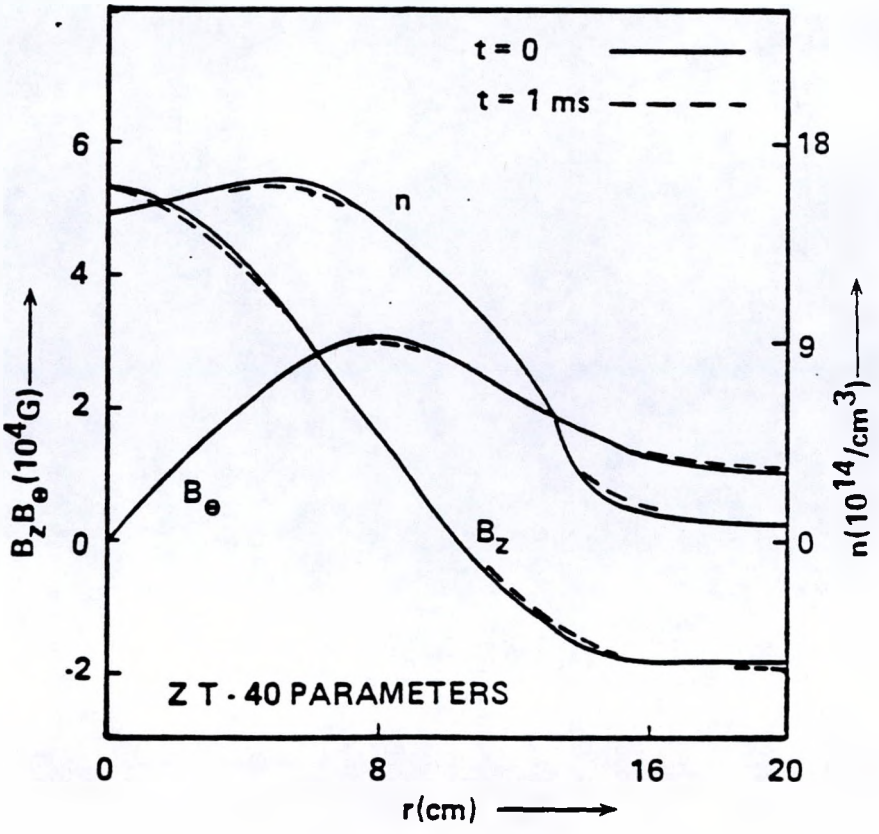

FIGURE 5b

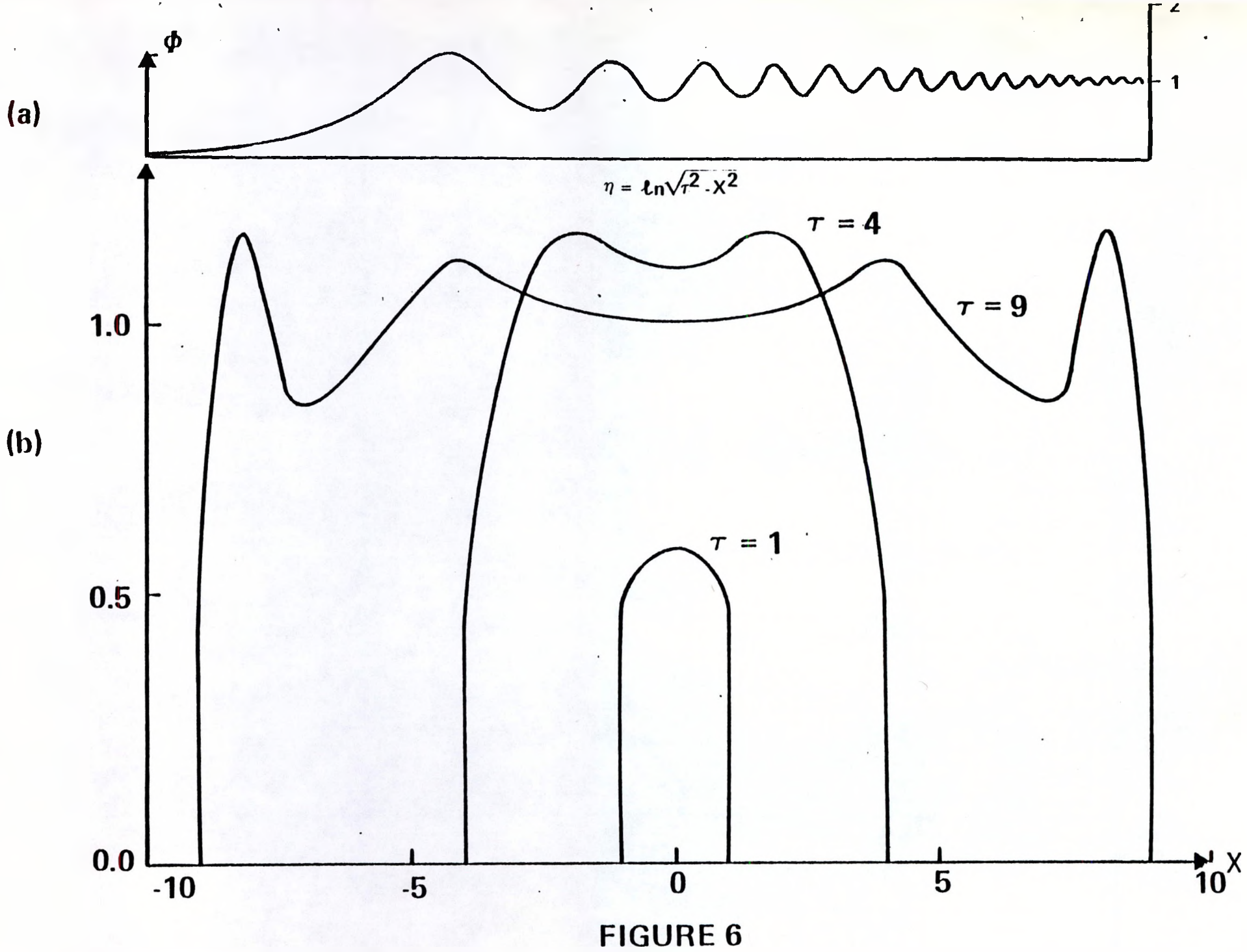

FIGURE 6

Space—Time Solution of the Nonlinear Partial Differential Equation